Polypeptide-guided assembly of conducting polymer nanocomposites

Mahiar Hamedi, Jens Wigenius, Feng-i Tai, Per Björk and Daniel Aili

Original Publication:

Mahiar Hamedi, Jens Wigenius, Feng-i Tai, Per Björk and Daniel Aili, Polypeptide-guided assembly of conducting polymer nanocomposites, 2010, NANOSCALE, (2), 10, 2058-2061.
http://dx.doi.org/10.1039/c0nr00299b

ARTICLE TYPE www.rsc.org/xxxxxx | XXXXXXXX

Polypeptide-Guided Assembly of Conducting Polymer Nanocomposites

Mahiar Hamedi,[a] Jens Wigenius,[a] Feng-I Tai,[b] Per Björk,[a] Daniel Aili*[,b,c]

Received (in XXX, XXX) Xth XXXXXXXXX 200X, Accepted Xth XXXXXXXXX 200X
First published on the web Xth XXXXXXXXX 200X
DOI: 10.1039/b000000x

A strategy for fabrication of electroactive nanocomposites with nanoscale organization, based on self-assembly is reported. Gold nanoparticles are assembled by a polypeptide folding-dependent bridging. The polypeptides are further utilized to recruit and associate with a water soluble conducting polymer. The polymer is homogenously incorporated into the nanocomposite, forming conducting pathways which makes the composite material highly conducting.

The development of nanoelectronics has resulted in enormous advancements in fabrication techniques that have enabled mass-production of CMOS circuits with feature sizes below 45nm.[1] There is a large interest in new methods to further push the size limits, lower the production costs and to facilitate the design of more advanced three-dimensional structures beyond today's 2.5 dimensional architectures. Self-assembly is probably the most important scheme in this development and is currently applied to many different areas and classes of nanoelectronics.[2] This technique enables fabrication of structures well below 10 nm in feature size and allows for incorporation of novel nanomaterials, such as metallic and semiconducting nanoparticles with many interesting optical and electrical properties.[3] The controlled self-assembly of electroactive nanocomposites is of great interest for the development of novel functional materials for biosensors,[4,5] electrochromic/plasmonic hybrid devices,[6] and polymer/nanoparticle-based memories.[7-9]

In the field of molecular self-assembly, biomolecules are widely employed as nanoscale building blocks because of their excellent molecular recognition properties, programmability, and chemical and structural versatility.[10] Biomolecules are, however, poor conductors and has consequently to be modified in order to be of interest for electronic applications. Water soluble conjugated/conducting polymers (CPs) that can associate to various biomolecules have been developed for this purpose. CPs that interacts with DNA has been employed to create supramolecular systems that mimic digital logic operations,[11,12] and for assembly of aligned luminescent nanowires.[13] In addition to DNA, proteins offer many interesting structural and chemical features and previously have been used as templates for assembly of CPs to obtain nanoelectronic functionalities.[14] Most proteins are however very fragile and can easily and irreversibly lose their native conformation, which severely limits their applicability as scaffolds for CPs. One inherently very stable protein structural state is the amyloid fibril. Amyloid-like protein fibrils have shown strong affinity for certain classes of ionic

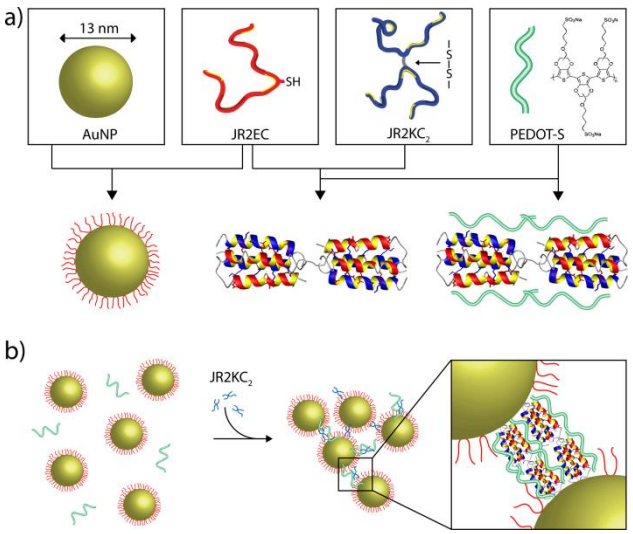

Fig. 1 a) Schematic illustration showing the basic nanoscale building blocks (from left to right): gold nanoparticles (AuNP), the designed polypeptides JR2EC and $JR2KC_2$, and the conducting polyelectrolyte PEDOT-S. JR2EC is immobilized on the gold nanoparticles via a thiol residue in the loop region. Two JR2EC monomers can heteroassociate with $JR2KC_2$ and fold into two disulphide-linked four-helix bundles, which can be utilized for assembly of JR2EC-decorated gold nanoparticles. The heterotrimeric complex is utilized as a scaffold for PEDOT-S for self-assembly of a conducting nanocomposite as illustrated in b).

CPs, which has enabled self-assembly of luminescent and conducting CP-amyloid nanowires.[15-17] The growth of amyloid fibres is however not easily controlled and often results in fibres with broad size distributions. Moreover, they are also not easily combined with other materials for assembly of more complex hybrid/composite nanostructures. In this perspective, the use of designed polypeptides with controllable assembly and folding properties seems very attractive. Polypeptides are generally extremely robust and are in terms of chemical and structural properties very flexible, which facilitate their use as molecular building blocks in nanoscale architectures.

In this communication we demonstrate a novel method for self-assembly of a water soluble conducting polymer (PEDOT-S) into supramolecular nanocomposites using well defined nanoscale building blocks comprised of designed synthetic polypeptides and polypeptide decorated gold nanoparticles as schematically outlined in Fig. 1. The two

synthetic polypeptides used here, JR2E and JR2K, are 42-residue polypeptides that are *de novo* designed to fold into a helix-loop-helix motif and heterodimerize into four-helix bundles at neutral pH.[18-21] At neutral pH, the glutamic acid rich polypeptide JR2E has a net charge of -5 whereas JR2K is rich in lysine residues and has a net charge of +11. Charge repulsion prevents homodimer formation at pH 7 and the peptide exists as random coil monomers when kept separate.[18,19] Incorporation of a cysteine residue in the loop region (position 22) yielded the polypeptides JR2EC and JR2KC. The thiol group enabled specific and site directed immobilization of JR2EC on planar gold surfaces,[19] and gold nanoparticles.[22,23] The cysteine-containing peptides can also exist in an oxidized form where two monomers are linked through a disulphide bond. The oxidized peptides, $JR2EC_2$ and $JR2KC_2$, can self-assemble into several micrometer long nanofibres as a result of hetero-association and folding into disulphide-linked four-helix bundles.[24] The fibre length can be controlled by capping the fibre growth using peptides without the cysteine residue. We have recently demonstrated that these fibres can be decorated with luminescent conjugated polymers.[25] Addition of $JR2KC_2$ to gold nanoparticles decorated with JR2EC results in a reversible heteroassociation and folding-dependent bridging of the nanoparticles.[26] The polypeptides were prepared on the solid phase and purified on HPLC as described in supporting information.

The conducting polymer poly(3,4-ethylenedioxythiophene) (PEDOT) is among the most stable class of highly conducting CPs. In the present study, a new generation of this polymer, alkoxysulfonate poly(3,4-ethylenedioxythiophene) (PEDOT-S), is utilized (Fig. S1).[27] PEDOT-S is self-doped in pristine state with conductivities above 1 S/cm. The anionic side chains make the polymer soluble in water and facilitate the interaction with various biomolecules. PEDOT-S has previously been demonstrated to assemble onto preformed amyloid fibrils forming conducting nanowire networks and transistors.[28]

Circular dichroism (CD) spectroscopy was employed in order to initially analyze the interaction between PEDOT-S and the polypeptides and the influence of PEDOT-S on the secondary structure of the polypeptides during self-assembly (Fig. 2a). When kept separately, JR2E and JR2K displayed typical random coil CD spectra. In the presence of PEDOT-S at a 1:1 molar ratio (50 μm), JR2K demonstrated a small increase in helicity whereas JR2E remained as a random coil. The interaction between PEDOT-S and the lysine rich JR2K is presumably mainly electrostatic resulting in enough shielding of charge repulsion between the polypeptide monomers to allow for a certain extent of folding. Folding of JR2K in the presence of a negatively charged CP has previously been reported.[18] In the absence of PEDOT-S, heterodimerization results in a mean residue molar ellipticity at 222 nm ($[\Theta]_{222nm}$) of about -21000 deg cm^2 $dmol^{-1}$. Addition of JR2K to a suspension of JR2E and PEDOT-S did not significantly affect the helicity, demonstrating that the peptides are able to fold properly in the presence of the polymer. If instead allowing

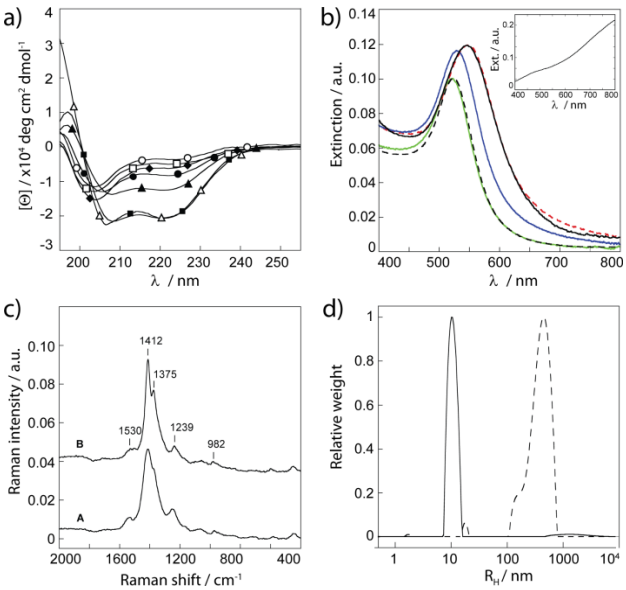

Fig. 2 a) CD-spectra of JR2E and JR2K at pH 7 in the presence and absence of PEDOT-S. (○) JR2E, (□) JR2E+PEDOT-S, (♦) JR2K, (●) JR2K+PEDOT-S, (▲) JR2K+PEDOT-S+JR2E, (■) JR2E+PEDOT-S+JR2K and (△) JR2E+JR2K. b) UV-vis-spectra of (black broken line) AuNP-JR2EC, (green) AuNP-JR2EC+PEDOT-S, (blue) AuNP-JR2EC+PEDOT-S+ $JR2KC_2$, (black) AuNP-JR2EC+ $JR2KC_2$+PEDOT-S, (red broken line) AuNP-JR2EC+ $JR2KC_2$. Inset: PEDOT-S. c) Raman spectra of A: PEDOT-S and B: AuNP-JR2EC+PEDOT-S+$JR2KC_2$, casted and dried on a glass substrate. d) Size distributions from DLS of (solid line) AuNP-JR2EC and PEDOT-S and (broken line) AuNP-JR2EC+PEDOT-S+$JR2KC_2$.

JR2K to first interact with PEDOT-S before introducing JR2E, a significantly lower helicity was obtained, $[\Theta]_{222nm}$ ~ -14500 deg cm^2 $dmol^{-1}$. This indicates that PEDOT-S can associate to the JR2K monomers and affect their ability to heterodimerize and fold. The concentration of the peptides was assumed to be constant during measurements as no aggregation or precipitation was observed.

Gold nanoparticles with an average diameter of ~13 nm were prepared by reduction of gold chloride with sodium citrate in aqueous solution.[29] JR2EC was immobilized on the particles via the thiol residue in the loop region and unbound peptides were removed by repeated centrifugations. Spherical gold nanoparticles display a pronounced extinction band in the visible wavelength range due to the localized surface plasmon resonance (LSPR). A small shift in the LSPR peak position, from ~520 nm to ~524 nm, was seen after addition of the peptide, indicative of a successful immobilization. In the presence of PEDOT-S, these particles remained dispersed and no further changes in the LSPR peak were seen (Fig. 2b). This further confirms the observations from the CD-spectrum of JR2E and PEDOT-S that no interactions between the two molecules occur and that the unspecific association of PEDOT-S to the gold nanoparticles is negligible. This is most likely due to the strong electrostatic charge repulsion between the two highly negatively charged species. The UV-vis

spectrum of aqueous PEDOT-S dispersion typically shows a pale blue colour characterized by a broad bi-polaron absorption between 600 and 1000 nm, often referred to as a "free carrier tail" (Fig. 2b, inset).[30] No changes in the spectra of PEDOT-S were seen in the presence of the peptides or peptide-decorated gold nanoparticles (data not shown), and the absorption of PEDOT-S was for clarity subtracted from the presented UV-vis spectra of the gold nanoparticles.

Aggregation of gold nanoparticles results in a substantial redshift of the LSPR peak position as well as a peak broadening, caused by the near-field coupling between adjacent particles. The magnitude of the redshift is highly dependent on the particle separation and the size of the aggregates. The smaller the distance and the larger the aggregates, the larger the resulting redshift.[31,32] Specific and controlled aggregation of the JR2EC decorated particles can be induced in a number of ways by exploiting the folding properties of the peptides. A rapid and extensive particle aggregation is observed in the presence of $JR2KC_2$ due to a heteroassociation- and folding-dependent bridging of the particles.[26] The resulting optical shift ($\Delta\lambda$ > 30 nm) was not influenced by addition of PEDOT-S after addition of $JR2KC_2$. Addition of PEDOT-S before addition of $JR2KC_2$ also resulted in extensive particle aggregation but the resulting redshift was less pronounced ($\Delta\lambda$ ~ 10 nm), indicating either a larger particle separation upon aggregation or smaller aggregates (Fig. 2b). The particles eventually precipitated, resulting in a colourless solution and a purple precipitate, suggesting the presence of large aggregates. UV-vis spectra of the supernatant showed no presence of PEDOT-S indicating that all of the PEDOT-S had associated to the peptides. This was further confirmed by Raman spectroscopy (Fig. 2c). In the Raman spectrum of PEDOT-S, one strong peak at 1412 cm^{-1} and a few weaker bands were observed. The peaks are assigned as follows: 1530 cm^{-1} (asym C=C str, sym C_α=C_β(-H) str), 1412 cm^{-1} (sym C_α=C_β(-O) str), 1239 cm^{-1} (C_α–C_α´(inter ring) str) + C_β-H bend, 986 cm^{-1} (oxyethylene ring def).[33] An almost identical spectrum, but showing a slightly narrower band at 1412 cm^{-1}, was obtained for the nanocomposite, demonstrating that the polymer was present in the composite and that its structure was not significantly affected by the association to the polypeptides.

Dynamic light scattering experiments further confirmed that gold nanoparticles functionalized with JR2EC did not assemble with PEDOT-S until after addition of $JR2KC_2$ (Fig. 2d). In aqueous solution, PEDOT-S mainly exists as single chains or aggregates of only a few polymer chains.[27] Dispersions of PEDOT-S and the JR2EC modified particles showed a rather narrow size distribution with a hydrodynamic radius of approximately 10 nm, mainly reflecting the size of the peptide functionalized particles as the particles are significantly better scatterers than the dispersed polymer. The addition of $JR2KC_2$ shifted and broadened the size distribution to about 500 nm within 5 minutes, indicating rapid initiation of the self-assembly process and extensive particle aggregation (Fig. 2d).The normalized autocorrelation functions are presented in Fig. S2. DLS also confirmed the interaction of $JR2KC_2$ with PEDOT-S, as assemblies with a broad size distribution and an average hydrodynamic radius of 150 nm were observed (Fig. S2).

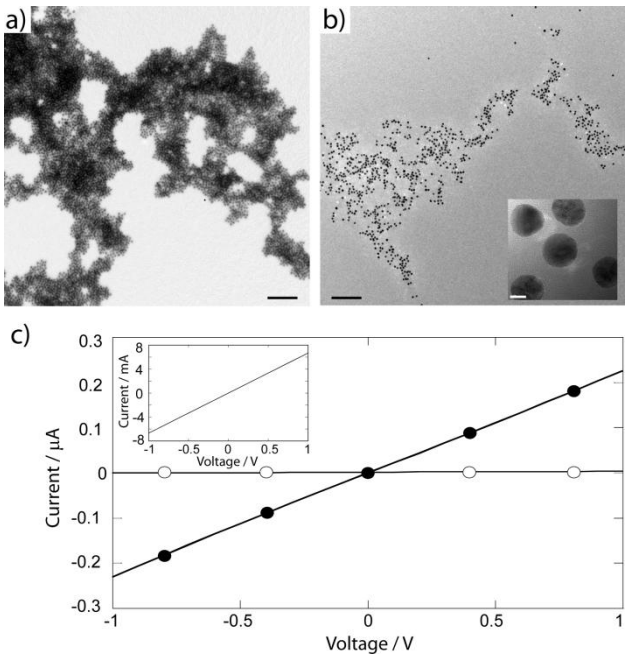

Fig. 3 Electron micrographs of the self-assembled nanocomposites a) without PEDOT-S and b) with PEDOT-S. Scale bars: 200 nm, inset 5 nm. c) Current-voltage characteristics of the nanocomposites (○) without PEDOT-S and (●) with PEDOT-S as measured on interdigitated gold electrodes. Inset: Current-voltage characteristics of pure PEDOT-S.

Transmission electron microscopy (TEM) was used to analyze the structure of the nanocomposites. In the absence of PEDOT-S, large aggregates with a small and uniform interparticle separation (4.6±0.2 nm) were seen (Fig. 3a). This is a consequence of the folding dependent bridging when $JR2KC_2$ associates with the immobilized JR2EC.[27] Addition of $JR2KC_2$ to a suspension of JR2EC functionalized nanoparticles containing PEDOT-S also resulted in large particle aggregates with a slightly larger and less uniform interparticle separation (Fig. 3b), as was indicated by the UV-vis spectra. The association of PEDOT-S to the peptides thus clearly affects the assembly of the particles resulting in less organized aggregates. This is presumably due to the association of PEDOT-S to $JR2KC_2$ which, as was indicated in the CD spectra, may induce a certain extent of homoassociation of the polypeptides and consequently an increase in particle separation. The conducting nature of PEDOT-S allows for larger assemblies of the polymer to be visualized directly in TEM.[28] No aggregates of PEDOT-S were however observed here (Fig. 3b), further indicating that the polymer is evenly distributed in the nanocomposite.

Conductivity measurements of the composite material were

carried out by casting the self-assembled structures from water solution onto inter-digitized gold electrodes, followed by measurement of current-voltage characteristics (CV). The same technique was utilized when depositing the nanocomposites on the electrodes as on the TEM-grids, resulting in very thin films. The gold nanoparticle-polypeptide complex alone did not show any conductivity because of the separation (~5 nm) between the gold nanoparticles induced by the non-conducting four-helix bundles (Fig. 3c). Despite displaying less dense assemblies, the PEDOT-S-containing nanocomposite was clearly conducting. Fully ohmic conductivity behaviour was seen for up to 1 V sweeps. The ohmic behaviour suggests that PEDOT-S remained conducting after the self-assembly process, and that the CP did not undergo noticeable oxidation/reduction during the voltage sweeps. As no unspecific binding of PEDOT-S to the particles was observed (Figure 2), this strongly indicates that the resulting electrical conductivity throughout the bulk structure is a result of the association of PEDOT-S to the heterotrimeric polypeptide complex, which provide conducting nanobridges between the gold nanoparticles. The overall conduction should hence be a combined result of inter-chain, and intra-chain hopping in the CP chains, as well as conduction through the gold nano particles and electron transfer between the gold nanoparticle and CPs. The conductivity was lower in the nanocomposite than when casting pure PEDOT-S on the electrodes (Fig. 3c, inset), which most likely is due to the lower amount of PEDOT-S present in the composite materials as compared to in the pure polymer solution as well as to the resistance at the polymer-nanoparticles interface.

Conclusions

The controlled self-assembly of highly conducting conjugated polymers (CPs) into a supramolecular electroactive nanocomposites using synthetic designed polypeptides and polypeptide decorated gold nanoparticles has been demonstrated. The polypeptide functionalized gold nanoparticles are assembled using a second set of polypeptides designed to heteroassociate and fold with the immobilized polypeptides. The CPs further associate to the polypeptides without significantly affecting their secondary structure, resulting in formation of extensive conducting networks. The proposed strategy for fabrication of electroactive nanocomposites enables a high level of control over the assembly process and the spatial arrangement of the nanoscale building blocks, as well as a large flexibility with respect to material composition. An efficient integration of conducting polymers into well defined nanocomposites will facilitate the development of novel components for bioorganic electronics, optoelectronics and biosensors and enable means for realizing an electronic interface at the nanoscale.

Acknowledgements: The authors thank Roger Karlsson for kindly providing the PEDOT-S, and Prof. Lars Baltzer, Dr. Johan Rydberg and Dr. Karin Enander for introducing us to the field of synthetic polypeptides, and Anna Herland for discussions. Financial support from the Knut and Alice Wallenberg Foundation (KAW), Forum Scientium, the Swedish Research Council (VR) and the Strategic Research Foundation (SSF) through the OBOE centre and the programmes OPEN and NanoSense is also gratefully acknowledged. The Authors are grateful for the support from Prof. Olle Inganäs and Prof. Bo Liedberg.

Notes and references

[a] *Division of Biomolecular and Organic Electronics Department of Physics, Chemistry and Biology, Linköping University, SE-581 83 Linköping, Sweden.*
[b] *Division of Molecular Physics, Department of Physics, Chemistry and Biology, Linköping University, SE-581 83 Linköping, Sweden. E-mail: danai@ifm.liu.se*
[c] *Current address: Department of Materials and Institute of Biomedical Engineering, Imperial College London, SW7 2AZ London, UK*
† Electronic Supplementary Information (ESI) available: Structure of PEDOT-S, DLS data and experimental details. See DOI: 10.1039/b000000x/

1 ITRS. (2010). I*nternational technology roadmap for semiconductors 2009 edition.* Available: http://www.itrs.net/Links/2009ITRS/Home2009.htm. Last accessed 22 mars.
2 G. M. Whitesides, B. Grzybowski, *Science*, 2002, **295**, 2418.
3 J. Li, *Curr. Opin. Colloid Interface Sci.*, 2009, **14**, 61.
4 R. Wilson, *Chem. Soc. Rev.*, 2008, **37**, 2028.
5 N. L. Rosi, C. A. Mirkin, *Chem. Rev.*, 2005, **105**, 1547.
6 M. A. G. Namboothiry, T. Zimmerman, F. M. Coldren, J. W. Liu, K. Kim, D. L. Carroll, *Synth. Met.*, 2007, **157**, 580.
7 R. J. Tseng, J. X. Huang, J. Ouyang, R. B. Kaner, Y. Yang, *Nano Lett.*, 2005, **5**, 1077.
8 G. Zotti, B. Vercelli, A. Berlin, *Chem. Mater.*, 2008, **20**, 6509.
9 A. Prakash, J. Ouyang, J. L. Lin, Y. Yang, *J. Appl. Phys.*, 2006, **100**, 054309.
10 N. C. Seeman, *Mol. Biotechnol.*, 2007, **37**, 246.
11 B. M. Frezza, S. L. Cockroft, M. R. Ghadiri, *J. Am. Chem. Soc.*, 2007, **129**, 14875.
12 Y. L. Tang, F. He, S. Wang, Y. L. Li, D. B. Zhu, G. C. Bazan, *Adv. Mater.*, 2006, **18**, 2105.
13 P. Björk, A. Herland, I. G. Scheblykin, O. Inganäs, *Nano Lett.*, 2005, **5**, 1948.
14 P. Björk, A. Herland, M. Hamedi, O. Inganäs, *J. Mater. Chem.*, 2010, **20**, 2269.
15 K. P. R. Nilsson, A. Herland, P. Hammarström, O. Inganäs, *Biochemistry*, 2005, **44**, 3718.
16 A. Herland, P. Björk, K. P. R. Nilsson, J. D. M. Olsson, P. Åsberg, P. Konradsson, P. Hammarström, O. Inganäs, *Adv. Mater.*, 2005, **17**, 1466.
17 A. Herland, P. Björk, P. R. Hania, I. G. Scheblykin, O. Inganäs, *Small*, 2007, **3**, 318.
18 K. P. R. Nilsson, J. Rydberg, L. Baltzer, O. Inganäs, *Proc. Natl. Acad. Sci. U. S. A.*, 2003, **100**, 10170.
19 K. Enander, D. Aili, L. Baltzer, I. Lundström, B. Liedberg, *Langmuir*, 2005, **21**, 2480.
20 S. Olofsson, L. Baltzer, *Fold. Des.*, 1996, **1**, 347.
21 S. Olofsson, G. Johansson, L. Baltzer, *J. Chem. Soc., Perkin Trans. 2*, 1995, 2047.
22 D. Aili, K. Enander, J. Rydberg, I. Nesterenko, F. Björefors, L. Baltzer, B. Liedberg, *J. Am. Chem. Soc.*, 2008, **130**, 5780.
23 D. Aili, K. Enander, J. Rydberg, I. Lundstrom, L. Baltzer, B. Liedberg, *J. Am. Chem. Soc.*, 2006, **128**, 2194.
24 D. Aili, F. I. Tai, K. Enander, L. Baltzer, B. Liedberg, *Angew. Chem., Int. Ed.*, 2008, **47**, 5554.
25 J. Wigenius, P. Björk, M. Hamedi, D. Aili, *Macromol. Biosci.*, 2010, **10**,836-841.
26 D. Aili, K. Enander, L. Baltzer, B. Liedberg, *Nano Lett.*, 2008, **8**, 2473.
27 R. H. Karlsson, A. Herland, M. Hamedi, J. A. Wigenius, A. Åslund, X. Liu, M. Fahlman, O. Inganäs, P. Konradsson, *Chem. Mater.*, 2009, **21**, 1815.
28 M. Hamedi, A. Herland, R. H. Karlsson, O. Inganäs, *Nano Lett.*, 2008, **8**, 1736.
29 G. Frens, *Nature (London) Phys. Sci.*, 1973, **241**, 20.
30 T. Kim, J. Kim, Y. Kim, T. Lee, W. Kim, K. S. Suh, *Curr. Appl. Phys*, 2009, **9**, 120.
31 U. Kreibig, MichelVollmer, *Optical Properties of Metal Clusters*, Vol. 25, Springer, New-York **1995**.
32 A. A. Lazarides, G. C. Schatz, *J. Phys. Chem. B*, 2000, **104**, 460.

33 S. Garreau, G. Louarn, J. P. Buisson, G. Froyer, S. Lefrant, *Macromolecules*, 1999, **32**, 6807.

Supporting Information

Polypeptide-Guided Assembly of Conducting Polymer Nanocomposites

Mahiar Hamedi,[a] Jens Wigenius,[a] Feng-I Tai,[b] Per Björk,[a] Daniel Aili*[b,c]

[a]*Division of Biomolecular and Organic Electronics Department of Physics, Chemistry and Biology, Linköping University, SE-581 83 Linköping, Sweden,* [b]*Division of Molecular Physics, Department of Physics, Chemistry and Biology, Linköping University, SE-581 83 Linköping, Sweden,* [c]*Department of Materials and Institute of Biomedical Engineering, Imperial College London, SW7 2AZ London, UK*

E-mail: danai@ifm.liu.se

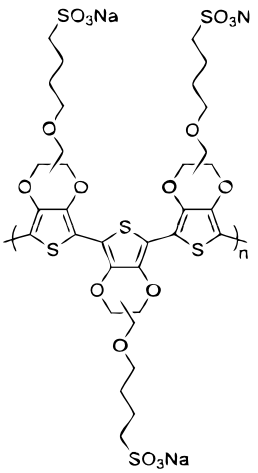

Fig. S1 Alkoxysulfonate poly(3,4-ethylenedioxythiophene) (PEDOT-S)

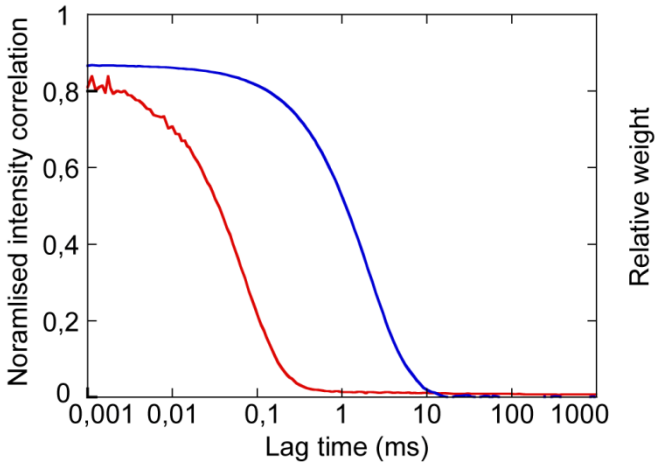

Fig. S2 Normalized intensity correlation for AuNP-JR2EC and PEDOT-S before (red) and after (blue) addition of the bridging polypeptide JR2KC$_2$. Hydrodynamic radius (R_h) of JR2KC$_2$ and PEDOT-S after 15 minutes incubation.

Experimental Details

Polypeptide and polymer synthesis: The polypeptides JR2E, JR2EC, (NAADLEKAIEALEKHLEAKGPCDAAQLEK QLEQAFEAFERAG), JR2K, and JR2KC (NAADLKKAIKALKKHLKAKGPCDAAQLK KQLKQAFKAFKRAG), were synthesized on a Pioneer automated peptide synthesizer (Applied Biosystems) using standard fluorenylmethoxycarbonyl (Fmoc) chemistry. The crude products were purified by reversed-phase HPLC on a semi-preparative HICHROM C-8 column and identified by MALDI-TOF mass spectrometry. In order to obtain JR2KC$_2$, lyophilized peptide monomers (1 mM) were dissolved in 0.1 M ammonium bicarbonate buffer pH 8, aerated for 90 minutes and incubated at 4^o C for at least 24 hours before use. Complete oxidation was confirmed using a standard Ellman´s test for determination of free thiols.[1] The synthesis of PEDOT-S is described in detail elsewhere.[2] The molar concentration of PEDOT-S was calculated based on an average molecular mass of 4000 g/mol, corresponding to approximately 12 monomer units.[2]

Nanoparticle synthesis and functionalization: Gold nanoparticles with an approximate average diameter of ~13 nm were prepared by citrate reduction of $HAuCl_4$. Details on synthesis are described elsewhere.[3] JR2EC (100 μM) in 10 mM sodium citrate pH 6 was incubated with the nanoparticles (~10 nM) for about 12 hours. Unbound peptides were removed by repeated centrifugations at 18000 g, and the supernatant was removed and replaced with 30 mM Bis-Tris buffer pH 7.0 until the resulting concentration of peptides in solution was less than 0.5 nM.

Structural analysis: Circular dichroism spectra were recorded with a CD6 Spectrodichrograph (JobinYvon-Spex) using a 0.1 mm cuvette at room temperature. Each spectrum was collected as an average of three scans in the range 190-260 nm. UV-vis spectroscopy was performed on a Schimadzu UV-1601PC spectrophotometer with 0.5 nm resolution at room temperature. TEM was conducted on a Philips CM20 Ultra-Twin lens high-resolution microscope operating at 200 kV.

20 μl of the samples was incubated on carbon coated TEM-grids for 2 minutes before the suspension was removed using a filter paper. The grids were dried before analysis. Dynamic light scattering experiments were carried out using an ALV/DLS/SLS-5022F system from ALV-GmbH, Langen Germany, using a HeNe laser at 632.8 nm with 22 mW output power at 90^{o}. Data analysis was carried out using the CONTIN 2DP routine implemented in the ALV data analysis package. Raman spectra were obtained using a FRA 106 Raman Fourier transform spectrometer (Bruker, Billerica, MA) equipped with a 1064 nm Nd:YAG laser and using a laser power of 400 mW and a 4 cm^{-1} resolution.

Current voltage measurements: The self-assembled structures were transferred to water and placed on an inter-digitized gold electrode with a spacing of 10 μm and a total length of 1 cm. The water was evaporated using a nitrogen flow flowed by washing with ethanol and water in order to removed ions and any unbound PEDOT-S from the surface.

References

1. G. L. Ellman, *Arch. Biochem. Biophys.*, 1959, **82**, 70-77.
2. R. H. Karlsson, A. Herland, M. Hamedi, J. A. Wigenius, A. Åslund, X. Liu, M. Fahlman, O. Inganäs, P. Konradsson, *Chem. Mater.*, 2009, **21**, 1815-1821.
3. D. Aili, K. Enander, J. Rydberg, I. Nesterenko, F. Bjorefors, L. Baltzer, B. Liedberg, *J. Am. Chem. Soc.*, 2008, **130**, 5780-5788.